J Membrane Biol (2010) 238:33–41
DOI 10.1007/s00232-010-9316-8

Bicarbonate Induces Membrane Reorganization and CBR1 and TRPV1 Endocannabinoid Receptor Migration in Lipid Microdomains in Capacitating Boar Spermatozoa

Laura Botto · Nicola Bernabò · Paola Palestini · Barbara Barboni

Received: 28 April 2010 / Accepted: 28 October 2010 / Published online: 23 November 2010

Abstract Mammalian spermatozoa acquire full fertilizing ability only after a morphofunctional maturation called "capacitation." During this process the high level of bicarbonate present within the upper female genital tract or in culture medium induces a marked reorganization of sperm membranes characterized by a biphasic behavior: In a few minutes, it promotes membrane phospholipid scrambling preliminary to the apical translocation of sterol that, 2–4 h later, enables spermatozoa to recognize zona pellucida after albumin-mediated cholesterol extraction. In the present research it was demonstrated that spermatozoa incubated with bicarbonate in protein-free media underwent a marked reorganization of lipid microdomains present in a detergent-resistant membrane fraction (DRM) isolated by ultracentrifugation on sucrose density gradient. In fact, bicarbonate exposed sperm (ES) cells, compared with ejaculated spermatozoa (nonexposed sperm [nES] cells), displayed an increase in protein DRM content and, in particular, in Cav-1 and CD55, markers of caveolae and lipid rafts, as well in acrosin-2, a marker of the outer acrosomal membrane (OAM). Moreover, the amount of certain proteins involved in capacitation, such as the endocannabinoid system receptors cannabinoid receptor type 1 (CBR1) and transient receptor potential cation channel 1 (TRPV1), increased in DRM obtained from ES. These data allow us to hypothesize that sperm membrane reorganization takes place even in the absence of extracellular proteins; that not only the plasma membrane but also the OAM participate in this process; and that important molecules playing a key role in inside–out signaling, such as the endocannbinoid receptors TRPV1 and CBR1, are involved in this event, with potentially important consequences on sperm function.

Keywords Spermatozoa · Bicarbonate · Lipid microdomain · Endocannabinoid receptor · Boar

L. Botto · P. Palestini
Department of Experimental Medicine (DIMS), University of Milano-Bicocca, Via Cadore 48, 20052 Monza, Italy

N. Bernabò · B. Barboni (✉)
Department of Comparative Biomedical Sciences, University of Teramo, Piazza A. Moro 45, 64100 Teramo, Italy
e-mail: bbarboni@unite.it

Introduction

In mammals, the spermatozoa gain full fertilizing ability only after they reside for a relatively long period (from hours to days, depending on the species) within the female genital tract. During this time the male gametes undergo an important series of morphofunctional modifications, known as "capacitation," involving all the subcellular compartments. In particular, the sperm membranes change their architecture: The plasma membrane (PM) and the outer acrosome membrane (OAM) become more unstable and gradually acquire the ability to fuse with each other (Gadella 2008; Gadella et al. 2008) only when the glycoprotein coat of the oocyte, the zona pellucida (ZP), is met. As a consequence, the exocytosis of acrosomal content, the so-called acrosome reaction (AR), takes place.

At present, the biochemistry of sperm membrane reorganization is still poorly understood and the information now available consists of a two-step model (Flesch et al. 2001). In the presence of high levels of bicarbonate, a soluble adenylate cyclase (sAC) is activated, triggering the production of cAMP and activating protein kinase A (Chen et al. 2000). This cAMP-dependent pathway leads to the activation of phospholipid scrambling in the apical plasma

membrane via a still unclear pathway, facilitating the relocalization of cholesterol over the spermatozoa head (Gadella and Harrison 2002). Cholesterol redistribution seems to be a key event in the completion of sperm capacitation, and it is preliminary to the cholesterol extraction that takes place only in the presence of protein acceptors. As a consequence, the membranes change their physicochemical proprieties, the lipid disorder and the fluidity increase and PM and OAM fusion becomes possible.

This model has been confirmed by several investigations (Gadella 2008; Gadella et al. 2008), even if what happens in the interval between the bicarbonate-mediated lipid scrambling and the protein-dependent cholesterol extraction remains unexplained. In fact, the exposure of phosphatidylserine (PS) occurs very rapidly, being clearly detectable within 5 min and largely complete within 10 min; and the exposure of phosphatidylethanolamine (PE), albeit with slower kinetics, is completed in 30 min (Gadella and Harrison 2002). Successively, after 2–4 h, the protein-mediated cholesterol extraction leads to the completion of membrane rearrangement and to the acquisition of spermatozoa fertilizing ability. In addition, it has been recently proposed (Gadella 2008) that this process involves specific membrane domains. In fact, the existence of discrete lipid domains (also known as "lipid microdomains") enriched in cholesterol and sphingolipids that specifically compartmentalize the membrane has been proposed in mammalian sperm, as well as their involvement in the acquisition of fertilizing ability (Travis et al. 2001; Shadan et al. 2004; Van Gestel et al. 2005). The lipid composition confers to these lipid microdomains their characteristic biochemical properties such as insolubility in non-ionic detergent (Triton X-100) at 4°C and light buoyant density after centrifugation in a discontinuous sucrose gradient. At present, two common types of lipid microdomains have been proposed: caveolae and lipid rafts. Lipid rafts are flat domains rich in GPI-anchored proteins and glycosphingolipids (gangliosides) (Brown 2006) that rely on lipid–lipid interaction for their formation and detergent resistance (Linder and Naim 2009). Caveolae are smooth, flask-shaped, cell-surface invaginations whose formation seems to be dependent on caveolin oligomerization (Anderson 1998; Parton and Simons 2007).

The rearrangement of membrane structure seems to act as a modulator of signaling cascades involved in the capacitation process. For instance, the function of the endocannabinoid system, in several cellular systems, has been found to be modulated by membrane components (Dainese et al. 2007; Bari et al. 2008). Starting from this basis, the aim of this work was to clarify the biochemical events involving membrane architecture in spermatozoa exposed to bicarbonate before the occurrence of protein-mediated cholesterol extraction. In addition, the functional meaning of these events was explored, studying the biochemical relocalization of two endocannabinoid system receptors, cannabinoid receptor type 1 (CBR1) and transient receptor potential cation channel 1 (TRPV1), known to be involved in capacitation-related spermatozoa signaling.

Materials and Methods

Chemicals

The reagents used (analytical grade) and high-performance thin layer chromatography (HPTLC) plates (Kieselgel 60) were purchased from Merck (Darmstadt, Germany). Dulbecco's modified Eagle medium (DMEM), fetal bovine serum (FBS), trypsin, penicillin/streptomycin, 3-(cyclohexylamino)1-propanesulfonic acid (CAPS), 2-(*N*-morpholino)ethansulfonic acid (MES), phenylmethylsulfonyl fluoride (PMSF), antiprotease and horseradish peroxidase–labeled cholera toxin B subunit (HRP-CTB) were from Sigma (Milan, Italy). Primary antibodies against caveolin-1 (C2297) and flotillin-2 (610383) were from Transduction Labs (Lexington, KY). CD55 (sc-9156) and vanilloid receptor 1 (sc-20813) were from Santa Cruz Biotechnology (Santa Cruz, CA). Antibody against actin (A2066) was from Sigma. Antibodies against CBR1 (ab40860) and acrosin (ab1900) were from Abcam (Cambridge, UK). Antibody against GM130 (Golgi marker), clone-35, was from Becton Dickinson (Mountain View, CA). Secondary antibodies for enhanced chemiluminescence (ECL) detection were anti-mouse, anti-rabbit and/or anti-goat HRP conjugates from Pierce (Rockford, IL). All material for electrophoresis was from Bio-Rad (Milan, Italy).

Sperm Collection and Incubation

Semen samples were collected from three boars of proven fertility. After removal of seminal plasma by two centrifugations (800×*g*, 10 min), sperm samples were immediately processed for biochemical analysis (nonexposed sperm [nES]) or diluted in TCM 199 supplemented with 1.25 mM calcium lactate, 1.25 mM sodium pyruvate and 13.9 mM glucose (Maccarrone et al. 2005), to a final concentration of 2×10^8 spermatozoa/ml to expose in vitro the spermatozoa to the bicarbonate ion (exposed sperm [ES]). Incubation was carried out at 38.5°C in a 5% CO_2 humidified atmosphere for up to 4 h. The incidence of AR recorded before and after exposure to solubilized ZP for 30 min was used to ascertain the status of sperm capacitation reached by each sample using the FITC-PSA (*Pisum sativum* agglutinin) staining technique (Barboni et al. 1995; Bernabò et al. 2007). Only sperm samples displaying an incidence of spontaneous AR < 15% and of

ZP-induced AR ranging 35–45% were used for the following biochemical analyses.

Membrane-Enriched Fraction Preparation

The membrane-enriched fraction (MEF) was prepared according to Thaler et al. (2006). Briefly, suspensions of nES or ES were pelleted (1,000×*g*, 15 min) and the supernatant was removed. Then, spermatozoa were washed in M2 salts (94.66 mM NaCl, 4.78 mM KCl, 1.19 mM KH_2PO_4, 1.19 mM $MgSO_4$, 20.85 mM HEPES [pH 7.4]) and pelleted. The sperm pellet was resuspended in hypotonic buffer (2 mM Tris [pH 7.2], 12 mM NaCl) with protease inhibitors (10 µg/ml aprotinin, 10 µg/ml leupeptin, 1 mM PMSF). The sperm suspension was sonicated six times for 15 s on ice, with each pulse separated by 1 min. This was repeated twice, and the cells were homogenized by pipetting up and down. Following a low-speed spin (2,500×*g*, 15 min) to remove cell debris, the supernatant containing crude sperm membranes was collected and centrifuged for 60 min at 108,000×*g*, 4°C. The obtained pellet contained the MEF.

Soluble and Insoluble Fraction Preparation

The MEFs of nES and ES were utilized for membrane subfractionation. The membrane pellet was resuspended in MBS containing protease inhibitors, as above, and the protein content assayed. A proper volume corresponding to 1 mg cellular proteins was adjusted to 500 µl by mixing with MBS-containing protease inhibitors. MEF suspensions were placed on ice, and an equal volume of cold 2% Triton X-100 in MBS with protease inhibitors was added and mixed. Tubes were held on ice for 30 min. The cell lysate was centrifuged at 15,000×*g* for 30 min at 4°C to separate the supernatant (soluble fraction) from the pellet (insoluble fraction) containing the lipid microdomains (Simons et al. 1999).

Preparation of Detergent-Resistant Membrane Fraction

MEFs from nES and ES were submitted to purification of a detergent-resistant membrane fraction (DRM), which includes caveolae and lipid rafts. Flotation gradients were prepared as described by Thaler et al. (2006) with minor modifications. Briefly, MEFs were resuspended in MES-buffered saline (MBS: 25 mM MES [pH 6.5], 150 mM NaCl) containing protease inhibitors, as above. The protein content was assayed, and a proper volume corresponding to 2.5 mg cellular proteins was adjusted to 0.5 ml, mixing it with MBS containing protease inhibitors in order to maintain a constant protein/detergent ratio in all experiments. Membrane suspensions were placed on ice, and then an equal volume of cold 2% Triton X-100 in MBS with protease inhibitors was added and mixed. Tubes were held on ice for 30 min. The cell lysate was adjusted to 40% sucrose by mixing with an equal volume of 80% (w/v) sucrose in MBS lacking Triton X-100 and layered on the bottom of a centrifuge tube. The 40% sucrose/membrane preparation was overlaid successively with 5 ml of 30% sucrose and 3 ml of 5% sucrose. The flotation gradients were centrifuged at 250,000×*g* for 18 h at 4°C with an SW-41 rotor (Beckman Instruments, Fullerton, CA). Membrane components were visible near the 5%/30% sucrose gradient interface in both nES and ES membrane preparations. Ten fractions of 1 ml were collected from the top of the gradient and designated as fractions 1 (top) to 10 (bottom). Fractions 4 and 5 will be referred to as "DRM," fractions 6 and 7 will be referred to as "intermediate-density fractions" (IDFs) and fractions 8–10 will be referred to as "high-density fractions" (HDFs). All fractions collected from the gradient were subjected to further analysis. For this study, two independent gradients were prepared from nES and ES.

Protein Analysis

Aliquots of MEF, soluble and insoluble fractions and all fractions collected from the sucrose gradient were subjected to trichloroacetic acid precipitation as previously described (Palestini et al. 2002); and the protein content was quantified by a micro-BCA assay from Sigma. Thereafter, 50 µg of MEF, 20 µg of soluble and insoluble fractions and 20 µg of proteins collected from the gradient fractions were loaded on SDS-PAGE (12% polyacrylamide gel) and submitted to electrophoresis. Subsequently, proteins were transferred to membranes that were stained with Ponceau S to assess protein loading by densitometry (Bio-Rad Densitometry 710, program Quantity one) (Salinovich and Montelaro 1986; Moore and Viselli 2000; Daffara et al. 2004). We compared in our samples the densitometry of the whole lane for protein loading obtained from one control and one exposed sperm for soluble and insoluble membrane fractions and gradient fractions.

Blots were washed with PBS and subsequently blocked overnight in PBS-T/milk. After blocking, blots were incubated for 2 h with the primary antibody diluted in PBS-T/milk (anti-Cav1 1:100, anti-CD55 1:200, anti-Flot2 1:200, anti-TPVR1 1:200, anti-CBR1 1:200, anti-actin 1:1,000, anti-ACR2 1:200, anti-GM130 1:200) and then for 1.5 h with HRP-conjugated anti-rabbit/mouse/goat IgG (5,000–10,000-fold diluted in PBS-T/milk). Protein samples were obtained from three controls and three treated animals. We performed in parallel immunoblot analysis of samples from one control and one exposed sperm for soluble and insoluble membrane fractions and for gradient fractions. Proteins were detected by ECL with the Super

Signal detection kit (Pierce). Immunoblot bands were analyzed and quantified by Kodak Image Station 2000R interfaced with a Kodak Molecular Imaging Software (Kodak, Rochester, NY). The data reported for each protein are the mean of four immunoblots ± standard deviation (SD), with different exposure times, obtained from two independent sucrose gradients. The significance of the differences was determined using one-way ANOVA and *t*-test.

Lipid Analysis

All fractions withdrawn from the gradient were dialyzed against distilled water at 4°C and then lyophilized. Lipids were extracted according to Tettamanti et al. (1973) with small modifications. The organic phases of extracted lipid samples were separated by HPTLC (solvent system hexane/diethylether/acetic acid 20:35:1, v/v/v) for cholesterol visualization and, then, sprayed with anisaldehyde reagent. After heating the plate at 180°C for 15 min, HPTLC plates were submitted to densitometric scanning. Quantification was made on the basis of known amounts of standard lipids loaded on the same plate. In the case of G_{M1}, HPTLC separation of the aqueous phase, blotting with HRP-CTB, ECL detection and quantification were performed, using Molecular Analyst Software (Bio-Rad), as already described (Wu and Ledeen 1988; Botto et al. 2008). The data reported for the amount of cholesterol and G_{M1} in each sucrose gradient fraction are the mean of four HPTLC separations ± SD obtained from two independent sucrose gradients. The significance of the differences was determined using one-way ANOVA and *t*-test.

Results

The aim of the present research was to study the membrane reorganization process induced in boar spermatozoa during in vitro culture carried out in the presence of bicarbonate by focusing, in particular, on the modifications occurring within lipid microdomains (caveolae and/or lipid rafts) and their composition in endocannabinoid receptors (CBR1 and TRPV1).

The first experiment was performed using spermatozoa MEFs in order to evaluate the percentage of insoluble membrane components before and after bicarbonate stimulation.

The amount of Cav-1 (marker of caveolae) and CD55 (marker of lipid rafts) increased in the insoluble membrane fraction derived from in vitro incubated spermatozoa (from 35 and 20% to 60 and 70%, respectively), thus displaying a rise in the insolubility for both proteins (Fig. 1). By contrast, the cholesterol content (lipid marker) remained unmodified, showing about 48% in either nES or ES.

Successively, the lipid microdomains were separated from the MEF using the validated technique based on their insolubility in cold non-ionic detergent and the capacity of the DRM to float into the buoyant fractions of sucrose gradients during ultracentrifugation.

The total protein amount of each gradient fraction was analyzed and is reported in Fig. 2 in percentages: The highest protein content was recovered in HDF (>80%) independently of spermatozoa incubation. The total membrane protein content in DRM (fractions 4 and 5) was about 1.6% in nES and increased significantly to 2.3% in ES (Fig. 2a). In addition, a relevant increase in protein content was recorded in IDF.

In order to check the efficiency of DRM purification, the percentage distribution of cholesterol and G_{M1} ganglioside in the gradient fractions was considered (Fig. 3a, c). Both lipids were enriched in fractions 4 and 5, as expected; and their distribution within the gradient was unaffected by exposure to the bicarbonate ion. However, normalizing the lipid levels for the protein total content (n[p]mol lipid/mg

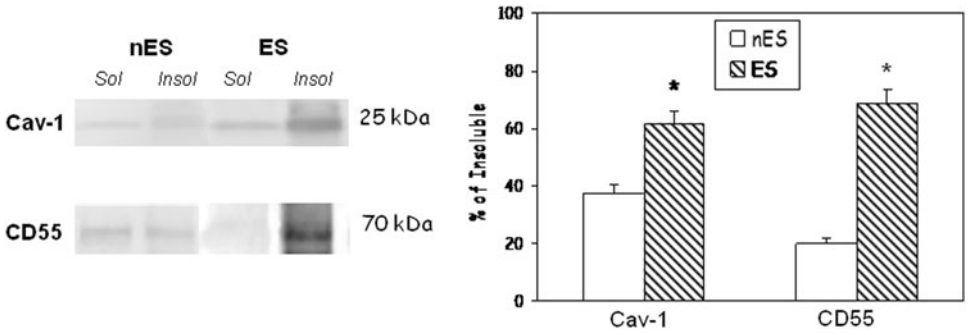

Fig. 1 Distribution of specific lipid microdomain protein markers between soluble and insoluble membrane fractions prepared from nES and ES. **a** Proteins extracted from soluble (*Sol*) and insoluble (*Insol*) membrane fractions were resolved on 12% SDS-PAGE and, after Western blotting, detected with anti-Cav1 and anti-CD55 antibodies, followed by ECL. **b** Percent of soluble and insoluble Cav1/CD55. Immunoblot bands were analyzed and quantified by Kodak Image Station 2000R interfaced with Kodak Molecular Imaging software. The data reported for each protein are the mean of four immunoblots ± SD, with different exposure times, obtained from two independent sucrose gradients. nES vs. ES $*P < 0.01$

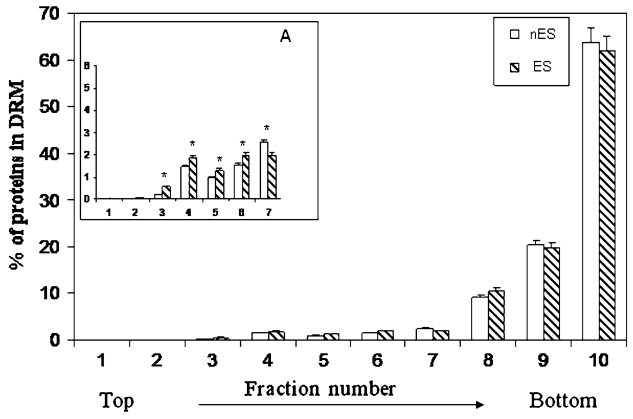

Fig. 2 Percentage distribution of proteins in DRM fractions prepared from MEFs obtained from nES and ES. MEFs were treated with 1% Triton X-100-containing buffer for 30 min on ice. The suspension was submitted to discontinuous sucrose density gradient centrifugation; ten fractions of 1 ml were collected from the top of the gradient and designated as fractions 1 (*top*) to 10 (*bottom*). Each fraction from the gradient was submitted to protein assay, and fractions 4 and 5 are referred to as "DRM." *Inset A* Percentage of proteins in fractions 1–7 using a different scale. Data are the mean of three protein determinations ± SD obtained from two independent sucrose gradients. nES vs. ES $*P < 0.05$

proteins; Fig. 3b, d), cholesterol and G_{M1} amount in fractions 4 and 5 significantly decreased in bicarbonate incubated spermatozoa. This result indicated that the lipid markers of DRM are enriched in fractions containing lipid microdomains even if their percent distribution did not change after bicarbonate exposure. This condition caused a significant decrease of total cholesterol and G_{M1} in all gradient fractions.

In addition, the proteins known to be enriched in lipid microdomains were analyzed. In detail, Cav-1 and CD55 (Fig. 4a, b) displayed a very similar distribution: In fact, both proteins were detectable only in HDF in nES, whereas their amount increased in DRM and IDF after sperm incubation. In contrast, the distribution of Flot-2, a protein enriched in both lipid microdomains (caveolae and lipid rafts), showed minor modification within the gradient (Fig. 4c) in sperm after bicarbonate exposure.

In order to exclude that the inadequate MEF purification technique and/or the presence of a high amount of inner membranes (i.e., Golgi), characterized by the presence of lipid microdomains "in assembling," were responsible for the anomalous distribution of lipid microdomain markers, additional membrane molecules were considered.

A good efficiency of MEF purification was confirmed by actin (cytosolic marker) levels that never exceeded 5% in nES or ES. Nevertheless, the high content in acrosin-2, an acrosomal membrane marker (99%), demonstrated that MEF included either inner or plasma membranes (data not shown). Then, in order to assess the acrosome contamination of DRM, the distribution of acrosin-2 in all gradient fractions was also evaluated. Figure 5 clearly shows how proteins were distributed in all gradients considered even if the amount markedly increased in DRM and IDF of ES.

In addition, the absence of Golgi membrane contamination in both nES and ES was confirmed using GM130 (data not shown).

Finally, the distributions of endocannabinoid receptors TRPV1 (Fig. 6a) and CBR1 (Fig. 6b) within gradient fractions obtained from nES and ES were analyzed. In nES, TRPV1 was exclusively localized in HDF and CBR1, even if mainly localized in fraction 10, was also distributed within DRM. After in vitro incubation, DRM was enriched in both CBR1 and TRPV1 and, interestingly, CBR1 was revealed by two different bands.

Discussion

The acquisition of fertilizing ability by mammalian spermatozoa is the result of a series of cellular interactions between the male gamete and the female genital tract. The completion of this process implies the reorganization of virtually all of the cellular components and, in particular, of membrane lipids and proteins. Following the explicative model until now available, it is possible to distinguish two different events related to membrane reorganization. First, membrane lipid disorder increases within 2 min and phospholipid scrambling takes place in a few minutes (Gadella and Harrison 2002). Second, after 2–4 h, protein-mediated cholesterol extraction leads to completion of membrane rearrangement and to acquisition of spermatozoa fertilizing ability. What physiologically happens in the interval between these events is still poorly understood. Our result seems to indicate that the bicarbonate could promote, in the absence of extracellular proteins, a massive membrane reorganization. First of all, in vitro incubated spermatozoa show an increase of DRM protein content. This process is associated with a significant increase of caveolae and CD55, a marker of lipid rafts, in insoluble membrane fractions, thus suggesting an increase of both lipid microdomains after bicarbonate exposure. These data are confirmed when fractions enriched in lipid microdomains (DRM) are obtained thanks to their insolubility in Triton X-100 at 4°C and separation after centrifugation in a discontinuous sucrose gradient (Botto et al. 2008). In addition, the percentage of cholesterol in insoluble membrane fractions and the percentage of cholesterol and G_{M1} in all gradient fractions are unchanged, thus demonstrating that this process is cholesterol extraction–independent. It is of interest to note that the data currently available, obtained from several laboratories (Boerke et al. 2008; Bou Khalil et al. 2006; Nixon and Aitken 2009; Shadan et al. 2004),

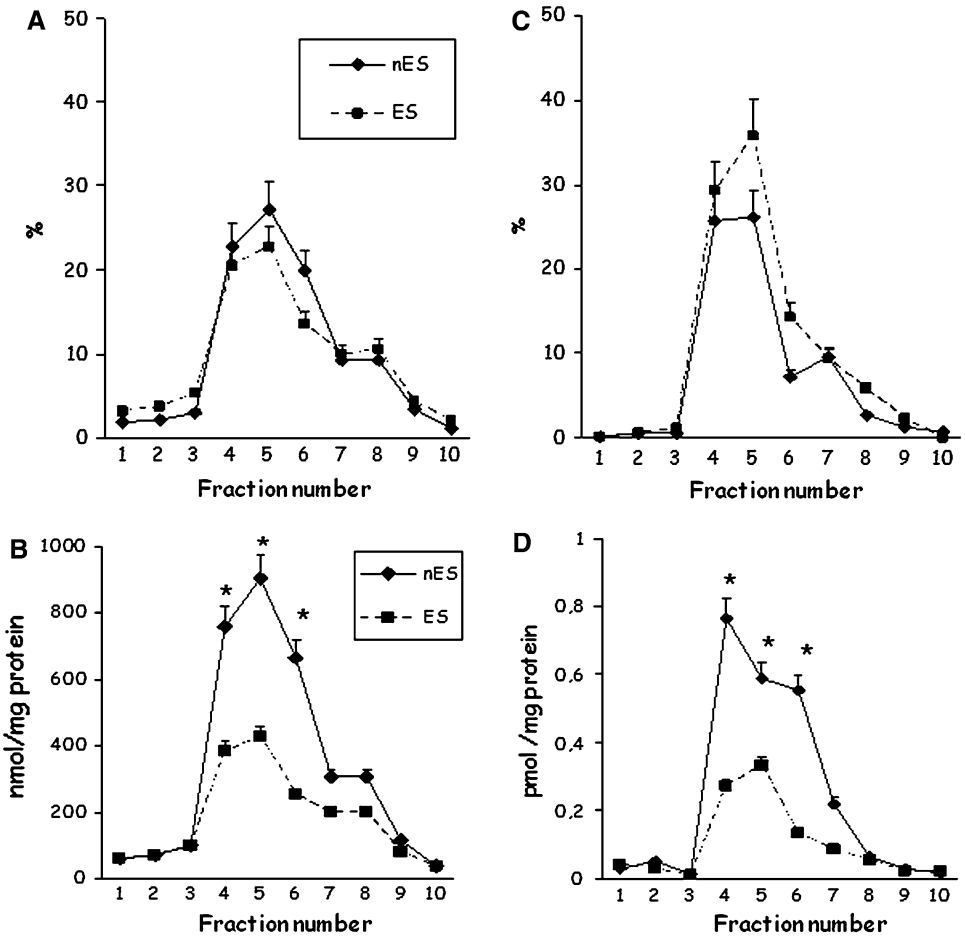

Fig. 3 Content of G_{M1} and cholesterol in sucrose density gradient fractions prepared from MEFs obtained from nES and ES. Lipids were extracted from all gradient fractions with chloroform/methanol 2:1 (v/v) and analyzed by HPTLC. Bands are quantified by densitometric scanning (see "Materials and Methods" section). **a**, **c** Percentage distribution of cholesterol and G_{M1} ganglioside in gradient fractions (1–10). **b**, **d** Amount of cholesterol and G_{M1} ganglioside, normalized to total protein content in gradient fractions (1–10) and expressed as nanomoles or picomoles per milligram proteins. Data are the mean of three lipid determinations ± SD obtained from two independent sucrose gradients. nES vs. ES $*P < 0.01$

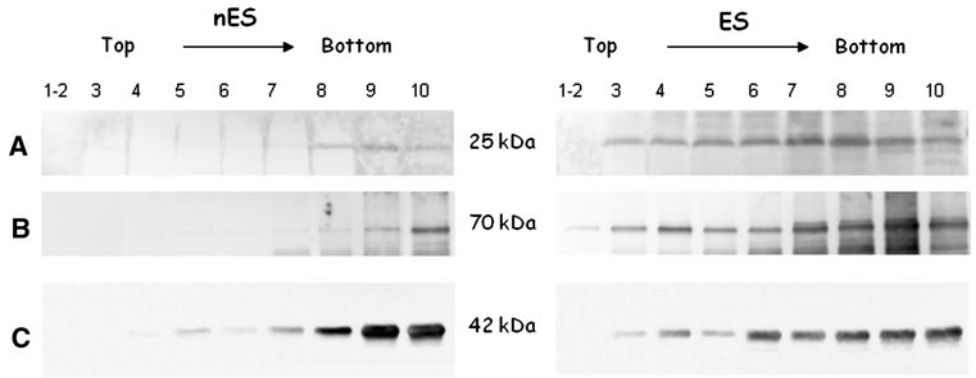

Fig. 4 Effects of capacitation on the content of Cav-1, CD55 and Flot2 in gradient fractions. Representative immunoblots of Cav-1 (**a**), CD55 (**b**) and Flot2 (**c**) in the various fractions obtained from discontinuous sucrose density gradient centrifugation of nES and ES. Twenty micrograms of proteins collected from all gradient fractions were loaded on SDS-PAGE (12% polyacrylamide gel) and submitted to electrophoresis and Western blotting. Immunoblot bands were analyzed by Kodak Image Station 2000R interfaced with Kodak Molecular Imaging software. *Numbers at top* indicate fraction number

indicate that capacitation implies a marked reorganization of membrane architecture when cholesterol is extracted by extracellular proteins. Until now, it was universally believed that microdomain remodeling can occur only in the presence of extracellular proteins (in most cases, albumin) or cholesterol-extracting molecules (e.g., β-methylcyclodextrin) (Choi and Toyoda 1998). In the present work, for the first time, it is proposed that the reorganization of DRM starts before the cholesterol extraction.

The behavior of protein markers Cav-1, Flot-2 and CD55 in DRM corroborates the hypothesis that bicarbonate

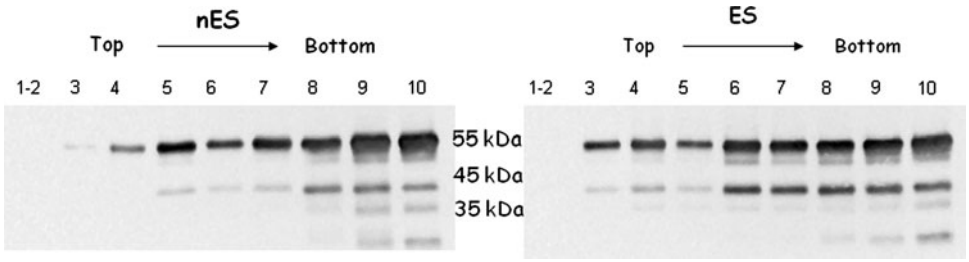

Fig. 5 Effects of capacitation on the content of acrosin-2 in gradient fractions. Representative immunoblots of acrosin-2 in the various fractions obtained from discontinuous sucrose density gradient centrifugation of nES and ES. Twenty micrograms of proteins collected from all gradient fractions were loaded on SDS-PAGE (12% polyacrylamide gel) and submitted to electrophoresis and Western blotting. Immunoblot bands were analyzed by Kodak Image Station 2000R interfaced with Kodak Molecular Imaging software. *Numbers at top* indicate fraction number

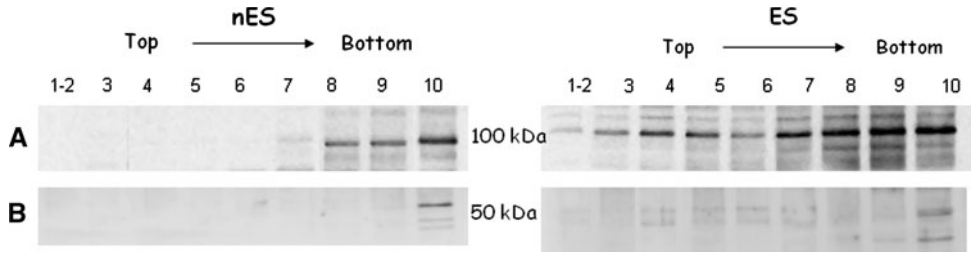

Fig. 6 Effects of capacitation on the content of endocannabinoid receptors in gradient fractions. Representative immunoblots of TRPV1 (**a**) and CBR1 (**b**) in the various fractions obtained from discontinuous sucrose density gradient centrifugation of nES and ES. Twenty micrograms of proteins collected from all gradient fractions were loaded on SDS-PAGE (12% polyacrylamide gel) and submitted to electrophoresis and Western blotting. Immunoblot bands were analyzed by Kodak Image Station 2000R interfaced with Kodak Molecular Imaging software. *Numbers at top* indicate fraction number

exposure induces an increase in the protein content of lipid microdomains, even if the distribution of these proteins in the gradient is atypical. In order to confirm this finding, insufficient purification of MEF or of DRM is excluded. In the first case, the efficiency of MEF extraction is confirmed by the absence of contamination by cytosolic proteins (actin). Adequate purification of DRM is indicated by the finding that 90% of membrane proteins are localized in HDFs of the gradient and lipid markers (cholesterol and G_{M1}) are significantly enriched in DRM.

Thus, a possible explanation of protein distribution within the gradient may be that MEF contains not only PM but also components from OAM: The Golgi membrane marker has not been found, while acrosin (marker of OAM) is present in all gradient fractions. Since the Golgi, and in particular the *trans*-Golgi, is the site of DRM assembly (Zegers and Hoekstra 1998; Schuck and Simons 2004) and the precursor of the acrosome (Burgos and Gutiérrez 1986; Ho et al. 1999; Huang and Ho 2006), it is possible to conceive that the acrosome membrane could contain a DRM fraction "in assembling."

Asano et al. (2009) demonstrated that in mouse sperm the presence of Cav-1 in different subtypes of lipid microdomains can reflect preferential contribution from specific subcellular organelles. Moreover, the demonstration that CD55, in human spermatozoa, is associated with both the PM and acrosome (Cummerson et al. 2006) strengthens the hypothesis that lipid microdomains, during their formation, are also present in the acrosome membrane.

Starting from these considerations, it is possible to hypothesize that some DRM component could originate from the acrosomal vesicle and be carried to the sperm surface via an exocytotic process after the spermatozoa are exposed to the bicarbonate. Thus, we proposed involvement of the OAM in membrane remodeling. These data have a logical explanation, considering that if the PM and OAM must fuse, at the moment of AR, the signaling machinery and reorganization must involve both components of the system.

Also, evidence that the membrane reorganization implies the biochemical reshaping of molecules, such as the CBR1 and TRPV1 endocannabinoid receptors involved in spermatozoa signaling pathways, emerges. The CBR1, from our data, is not enriched in lipid microdomains and localizes in HDFs but, after the bicarbonate exposure, undergoes a redistribution, increasing its content in DRM. In particular, it appears in

the form of a double band in DRM and IDF but not in HDF: a band at about 54 kDa, corresponding to the unglycosylated form, and one at about 65 kDa, corresponding to the glycosylated (mature) form (Howlett 1998). Whereas glycosylation is essential for receptor function (Onaivi et al. 1996), the percentage that increases in DRM after bicarbonate exposure (about 50% of the total) suggest an important role of CBR1 in the signaling pathways involved in AR. Recent findings (Maccarrone et al. 2005) seem to indicate that CBR1 acts via a cAMP-mediated pathway, slowing the membrane tendency to become unstable, thus avoiding the premature loss of acrosome integrity.

TRPV1 too is not enriched in DRM, but bicarbonate exposure induces its increase in lipid microdomains. This endocannabinoid–endovanilloid receptor has been shown to regulate spermatozoa transmembrane potential, intracellular calcium concentration and actin polymerization (Bernabò et al. 2010). Thus, it is not possible to exclude that the redistribution of these receptors in different biochemical contexts within the PM and/or acrosome is correlated to the spatiotemporal control of sperm–egg interaction. Until now it has been reported that CBR1 and TRPV1 are involved in the acquisition of fertilizing ability by modulation of important signaling pathways (the cAMP and ionic intracellular concentrations, respectively). Now, it is evident that, in turn, the process of membrane remodeling strongly influences the biochemical localization of these molecules, allowing us to hypothesize that there exists a more complex and integrated functional dialogue between membrane microdomain architecture and the endocannabinoid system.

From all of these data it is possible to increase the information about the events occurring after the bicarbonate-dependent activation of lipid reorganization. It emerges that in this window of time an important membrane reorganization takes place, involving the PM, the OAM and receptors involved in important signal-transduction pathways. Starting from this basis, it is possible to complete the schema proposed by Flesch et al. (2001), adding a new step, as depicted (Fig. 7). On the one hand, this could improve our understanding of the basics of capacitation biochemistry, while on the other hand, it could have possible application in diagnostic and therapeutic strategies in male reproduction.

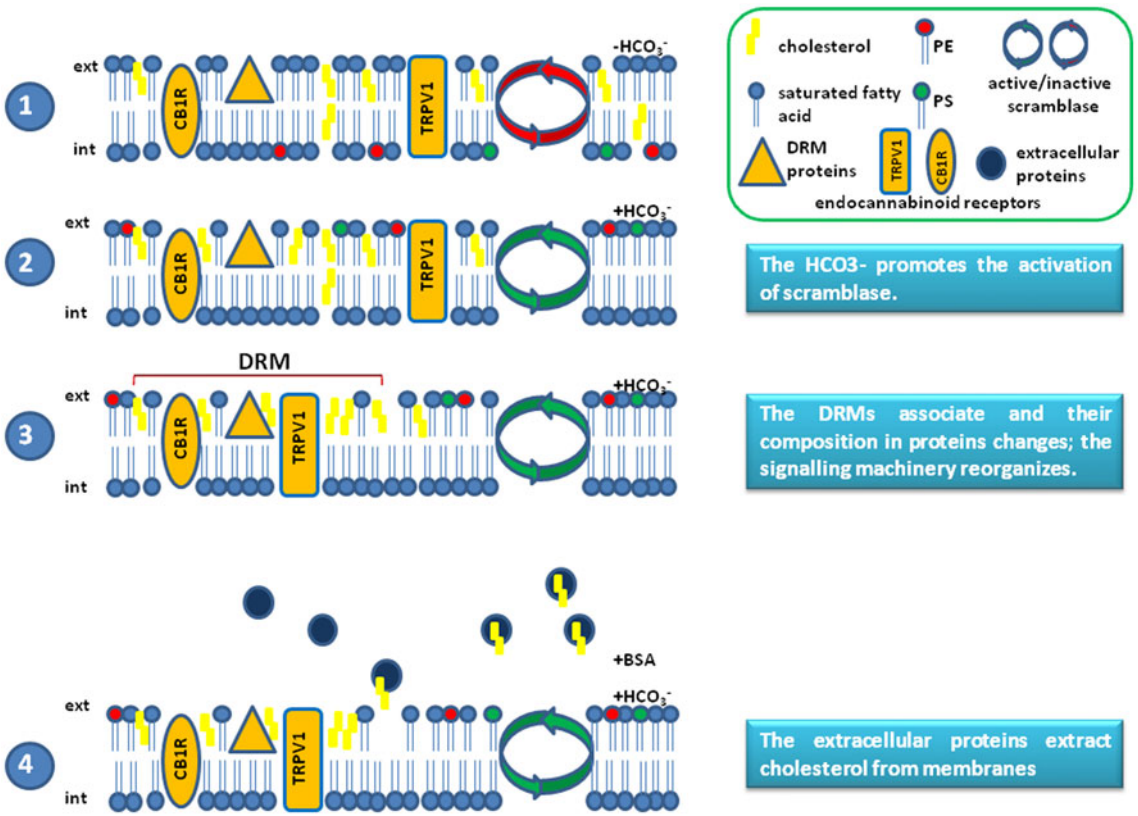

Fig. 7 Model for membrane reorganization in bicarbonate-stimulated sperm cells. *1* In the absence of high levels of bicarbonate, phospholipid scrambling is blocked. Cholesterol has a widespread lateral localization in the sperm head plasma membrane and DRM organization does not take place. *2* In the presence of high levels of bicarbonate, phospholipid scrambling is activated in the apical plasma membrane of the sperm head. *3* The DRMs associate and their content in proteins increases. The endocannabinoid system receptors associate to the DRMs. *4* The extracellular proteins extract cholesterol and the membrane completes its reorganization

References

Asano A, Selvaraj V, Buttke DE, Nelson JL, Green KM, Evans JE, Travis AJ (2009) Biochemical characterization of membrane fractions in murine sperm: identification of three distinct subtypes of membrane rafts. J Cell Physiol 218:537–548

Anderson RGW (1998) The caveolae membrane system. Annu Rev Biochem 67:199–225

Barboni B, Mattioli M, Seren E (1995) Influence of progesterone on boar sperm capacitation. J Endocrinol 144:1–8

Bari M, Oddi S, De Simone C, Spagnolo P, Gasperi V, Battista N, Centonze D, Maccarrone M (2008) Type-1 cannabinoid receptors colocalize with caveolin-1 in neuronal cells. Neuropharmacology 54:45–50

Bernabò N, Tettamanti E, Pistilli MG, Nardinocchi D, Berardinelli P, Mattioli M, Barboni B (2007) Effects of 50 Hz extremely low frequency magnetic field on the morphology and function of boar spermatozoa capacitated in vitro. Theriogenology 67:801–815

Bernabò N, Pistilli MG, Mattioli M, Barboni B (2010) Role of TRPV1 channels in boar spermatozoa acquisition of fertilizing ability. Mol Cell Endocrinol 323:224–331

Boerke A, Tsai PS, Garcia-Gil N, Brewis IA, Gadella BM (2008) Capacitation-dependent reorganization of microdomains in the apical sperm head plasma membrane: functional relationship with zona binding and the zona-induced acrosome reaction. Theriogenology 70:1188–1196

Botto L, Beretta E, Bulbarelli A, Rivolta I, Lettiero B, Leone BE, Miserocchi G, Palestini P (2008) Hypoxia-induced modifications in plasma membranes and lipid microdomains in A549 cells and primary human alveolar cells. J Cell Biochem 105:503–513

Bou Khalil M, Chakrabandhu K, Xu H, Weerachatyanukul W, Buhr M, Berger T, Carmona E, Vuong N, Kumarathasan P, Wong PT, Carrier D, Tanphaichitr N (2006) Sperm capacitation induces an increase in lipid rafts having zona pellucida binding ability and containing sulfogalactosylglycerolipid. Dev Biol 290:220–235

Brown D (2006) Lipid rafts, detergent resistant membranes and rafts targeting signals. Physiology 21:430–439

Burgos MH, Gutiérrez LS (1986) The Golgi complex of the early spermatid in guinea pig. Anat Rec 216:139–145

Chen Y, Cann MJ, Litvin TN, Iourgenko V, Sinclair ML, Levin LR, Buck J (2000) Soluble adenylyl cyclase as an evolutionarily conserved bicarbonate sensor. Science 289:625–628

Choi YH, Toyoda Y (1998) Cyclodextrin removes cholesterol from mouse sperm and induces capacitation in a protein-free medium. Biol Reprod 59:1328–1333

Cummerson JA, Flanagan BF, Spiller DG, Johnson PM (2006) The complement regulatory proteins CD55 (decay accelerating factor) and CD59 are expressed on the inner acrosomal membrane of human spermatozoa as well as CD46 (membrane cofactor protein). Immunology 118:333–342

Daffara R, Botto L, Beretta E, Conforti E, Faini A, Palestini P, Miserocchi G (2004) Endothelial cells as early sensors of pulmonary interstitial edema. J Appl Physiol 97:1575–1583

Dainese E, Oddi S, Bari M, Maccarrone M (2007) Modulation of the endocannabinoid system by lipid rafts. Curr Med Chem 14:2702–2715

Flesch FM, Brouwers JF, Nievelstein PF, Verkleij AJ, van Golde LM, Colenbrander B, Gadella BM (2001) Bicarbonate stimulated phospholipid scrambling induces cholesterol redistribution and enables cholesterol depletion in the sperm plasma membrane. J Cell Sci 114:3543–3555

Gadella BM (2008) Sperm membrane physiology and relevance for fertilization. Anim Reprod Sci 107:229–236

Gadella BM, Harrison RA (2002) Capacitation induces cyclic adenosine 3′,5′-monophosphate-dependent, but apoptosis-unrelated, exposure of aminophospholipids at the apical head plasma membrane of boar sperm cells. Biol Reprod 67:340–350

Gadella BM, Tsai PS, Boerke A, Brewis IA (2008) Sperm head membrane reorganisation during capacitation. Int J Dev Biol 52:473–480

Ho HC, Tang CY, Suarez SS (1999) Three-dimensional structure of the Golgi apparatus in mouse spermatids: a scanning electron microscopic study. Anat Rec 256:189–194

Howlett AC (1998) The CB1 cannabinoid receptor in the brain. Neurobiol Dis 5(6 Pt B):405–416

Huang WP, Ho HC (2006) Role of microtubule-dependent membrane trafficking in acrosomal biogenesis. Cell Tissue Res 323:495–503

Linder R, Naim HY (2009) Domains in biological membranes. Exp Cell Res 315:2871–2878

Maccarrone M, Barboni B, Paradisi A, Bernabò N, Gasperi V, Pistilli MG, Fezza F, Lucidi P, Mattioli M (2005) Characterization of the endocannabinoid system in boar spermatozoa and implications for sperm capacitation and acrosome reaction. Cell Sci 118:4393–4404

Moore MK, Viselli SM (2000) Staining and quantification of proteins transferred to polyvinylidine fluoride membranes. Anal Biochem 279:241–242

Nixon B, Aitken RJ (2009) The biological significance of detergent-resistant membranes in spermatozoa. J Reprod Immunol 83:8–13

Onaivi ES, Chakrabarti A, Chaudhuri G (1996) Cannabinoid receptor genes. Prog Neurobiol 48:275–305

Palestini P, Calvi C, Conforti E, Botto L, Fenoglio C, Miserocchi G (2002) Composition, biophysical properties and morphometry of plasma membranes in pulmonary interstitial edema. Am J Physiol Lung Cell Mol Physiol 282:1382–1390

Parton RG, Simons K (2007) The multiple faces of caveolae. Nat Rev Mol Cell Biol 8:185–194

Salinovich O, Montelaro RC (1986) Reversible staining and peptide mapping of proteins transferred to nitrocellulose after separation by sodium dodecyl sulphate-polyacrylamide gel electrophoresis. Anal Biochem 156:341–347

Schuck S, Simons K (2004) Polarized sorting in epithelial cells: raft clustering and the biogenesis of the apical membrane. J Cell Sci 117:5955–5964

Shadan S, James PS, Howes EA, Jones R (2004) Cholesterol efflux alters lipid raft stability and distribution during capacitation of boar spermatozoa. Biol Reprod 71:253–265

Simons M, Friedrichson T, Schulz JB, Pitto M, Masserini M, Kurzchalia TV (1999) Exogenous administration of gangliosides displaces GPI-anchored proteins from lipid microdomains in living cells. Mol Biol Cell 10:3187–3196

Tettamanti G, Bonali F, Marchesini S, Zambotti V (1973) A new procedure for the extraction, purification and fractionation of brain gangliosides. Biochim Biophys Acta 296:160–170

Thaler CD, Thomas M, Ramalie JR (2006) Reorganization of mouse sperm lipid rafts by capacitation. Mol Reprod Dev 73:1541–1549

Travis AJ, Merdiushev T, Vargas LA, Jones BH, Purdon MA, Nipper RW, Galatioto J, Moss SB, Hunnicutt GR, Kopf GS (2001) Expression and localization of caveolin-1, and the presence of membrane rafts, in mouse and guinea pig spermatozoa. Dev Biol 240:599–610

Van Gestel RA, Brewis IA, Ashton PR, Helms JB, Brouwers JF, Gadella BM (2005) Capacitation-dependent concentration of lipid rafts in the apical ridge head area of porcine sperm cells. Mol Hum Reprod 11:583–590

Wu C, Ledeen R (1988) Quantification of gangliotetraose gangliosides with cholera toxin. Anal Biochem 173:368–375

Zegers MM, Hoekstra D (1998) Mechanisms and functional features of polarized membrane traffic in epithelial and hepatic cells. Biochem J 336:257–269